Article

An Assessment of Marine Ecosystem Damage from the Penglai 19-3 Oil Spill Accident

Haiwen Han [1], Shengmao Huang [1], Shuang Liu [2,3,*], Jingjing Sha [2,3] and Xianqing Lv [1,*]

1   Key Laboratory of Physical Oceanography, Ministry of Education, Ocean University of China, Qingdao 266100, China; hanhaiwen@stu.ouc.edu.cn (H.H.); hsm4430@stu.ouc.edu.cn (S.H.)
2   North China Sea Environment Monitoring Center, State Oceanic Administration (SOA), Qingdao 266033, China; shajingjing@ncs.mnr.gov.cn
3   Department of Environment and Ecology, Shandong Province Key Laboratory of Marine Ecology and Environment & Disaster Prevention and Mitigation, Qingdao 266100, China
*   Correspondence: liushuang@ncs.mnr.gov.cn (S.L.); xqinglv@ouc.edu.cn (X.L.)

Abstract: Oil spills have immediate adverse effects on marine ecological functions. Accurate assessment of the damage caused by the oil spill is of great significance for the protection of marine ecosystems. In this study the observation data of *Chaetoceros* and shellfish before and after the Penglai 19-3 oil spill in the Bohai Sea were analyzed by the least-squares fitting method and radial basis function (RBF) interpolation. Besides, an oil transport model is provided which considers both the hydrodynamic mechanism and monitoring data to accurately simulate the spatial and temporal distribution of total petroleum hydrocarbons (TPH) in the Bohai Sea. It was found that the abundance of *Chaetoceros* and shellfish exposed to the oil spill decreased rapidly. The biomass loss of *Chaetoceros* and shellfish are $7.25 \times 10^{14} \sim 7.28 \times 10^{14}$ ind and $2.30 \times 10^{12} \sim 2.51 \times 10^{12}$ ind in the area with TPH over $50 \, \text{mg/m}^3$ during the observation period, respectively. This study highlights the evaluation of ecological resource loss caused by the oil spill, which is useful for the protection and restoration of the biological resources following the oil spill.

Keywords: Bohai Sea; oil spill; *Chaetoceros*; fish larvae; shellfish; biomass loss

1. Introduction

Marine environments are frequently exposed to oil spills as a result of transportation, oil drilling and fuel usage. An estimated 5000 tons of oil per year was spilled during the period 2010–2014 due to accidents, cleaning operations or other causes [1]. Crude oil constitutes a large reservoir of the highly toxic polycyclic aromatic hydrocarbons (PAHs), which are rapidly released into the water column after the spill. As we all known, oil slicks over the sea surface not only limit gas exchange through the air-sea interface, but also reduce light penetration into the water column, and resultant affecting the photosynthesis of phytoplankton [2]. The negative impact threatens the survival of marine life that feeds on phytoplankton. In addition, phytoplankton are the primary food source for the zooplankton, and are therefore the starting points for the entry of petroleum hydrocarbons into the marine food web [3,4]. Then the petroleum hydrocarbons are further enriched by marine organisms and amplified along the food chain, and ultimately harming human health due to their mutagenic or carcinogenic activity [5,6]. In general, oil spills not only affect the growth of marine organisms, disrupt the ecological mechanism and reproduction of the ocean [7,8], but also result in environmental and economic damage to fisheries and human health [9,10]. Therefore, accurate assessment of the damage caused by the oil spill is of great significance.

The impacts of oil spills on marine organisms have been studied over the past several decades, but the conclusions are often inconsistent. Batten et al. found phytoplankton community structure did not exhibit any significant differences before and after the spill [11].

Some studies have reported that phytoplankton are affected by the oil spill [12–15]. For example, Ohwada et al. found that an oil spill could result in a reduction in phytoplankton growth [16]. On the contrary, Guo et al. found that the oil spill caused abnormal chlorophyll concentration distributions which led to an outbreak of red tide [17]. The impact of oil spill on zooplankton is generally considered detrimental [18–20]. Gesteira and Dauvin noted that the benthic community structure could be altered by concentrations of petroleum hydrocarbons in sediment <50 ppm, and some species may be excluded at concentrations <10 ppm [21]. Therefore, the impact of oil pollution on marine ecosystems is a pendent and hot topic in the research field of ecological environment evaluation.

On 17 June 2011, an oil slick was detected in the offshore water near platform C of the Penglai 19-3 drilling field. The Penglai 19-3 oil spill was a typical Chinese oil spill, with some 115 m^3 of heavy crude oil and 416 m^3 of mineral oil-based drilling mud seeping into the Bohai Sea. To the best of our knowledge, studies examining its potential environmental impact are rare. In fact, the Bohai Sea, covering approximately 77,000 km^2 and surrounded by land on three sides, is the only semi-closed marginal sea in China. It connects to the Yellow Sea through the Bohai Strait. The limited water exchange capacity causes a poor self-purification ability of the Bohai Sea, making it difficult to restore in a short time if the marine ecosystem is severely damaged. Therefore, oil spill pollution is a serious threat to the Bohai Sea.

In this paper, an adjoint assimilation model of oil transport is established to simulate the spatial and temporal distribution of total petroleum hydrocarbons (TPH) in the Bohai Sea. Because observations in the oceans are often sparse and the oil spill movement still cannot be predicted by using only observation data. The oil transport model which provides scientific basis for oil spill prediction and emergency decision analysis [22–24] is an effective tool to simulate and forecast accurate spill trajectories under actual environmental conditions. In previous study, oil transport model has been successfully implemented for simulating oil slick trajectories and the temporal and spatial distribution of pollution [25–27]. The adjoint assimilation model can further simulate the real ocean scenario accurately through optimizing control parameters including initial conditions, boundary conditions and empirical parameters, which has been widely applied in oceanography for decades [28–36]. For example, Li et al. and Zheng et al. used the transport model to simulate the distribution of pollutants in the Bohai Sea [37,38]. Huang et al. used a model of transport and degradation to estimate the degradation coefficient of petroleum hydrocarbon pollutants [39].

In order to assess the effect of crude oil spill on marine biological community, the abundance of *Chaetoceros*, fish larvae and shellfish were monitored during June 15–July 13. The objectives of this paper are: (1) clarifying the changes in the abundance of *Chaetoceros*, fish larvae and shellfish after the oil spill; (2) exploring the relationship between the mortality and TPH; (3) evaluating the biomass loss caused by the oil spill based on radial basis function (RBF) interpolation and oil spill adjoint model.

2. Materials and Methods

2.1. Biological Observation Data

Based on monitoring result, the dominant species of the phytoplankton is *Chaetoceros* in the oil spill area. *Chaetoceros* played a major contribution of the total phytoplankton abundance in the short period after the oil spill [40]. Early life stages of fish are particularly vulnerable to oil spills [41]. In addition, the Bohai Sea is of great commercial importance as one of the major fishing areas in China [42]. Marine shellfish, such as mussels, have been widely used to monitor persistent organic pollutants (POPs) in coastal environments [43]. Therefore, *Chaetoceros,* fish larvae and shellfish serve as indicators of risk.

The *Chaetoceros*, fish larvae and shellfish distribution data near the Penglai 19-3 drilling field (120°06′ E, 38°23′ N) during 15 June–13 July was provided by the North China Sea Environmental Monitoring Center. The sampling and counting methods of *Chaetoceros* are vertical trawling sampling and the concentration counting method (The specification

for marine monitoring-Part 7: Ecological survey for offshore pollution and biological monitoring (GB 17378.7-2007)). The sampling and counting method of fish larvae are trawling sampling and direct counting method (Specifications for oceanographic survey Part 6: Marine biological survey (GB/T 12763.6-2007)). Shellfish was sampled by a bottom sampler and counted by direct counting method (The specification for marine monitoring-Part 7: Ecological survey for offshore pollution and biological monitoring (GB 17378.7-2007)). The sampling stations located in the area with the depth more than 20 m, and the biomass of three organisms were little affected by the tidal movements. The distribution of sampling stations is shown in Figure 1 and the locations of observations is given in Table 1. The oil spill was detected on 17 June 2011, while *Chaetoceros* and shellfish were observed before and after the oil spill.
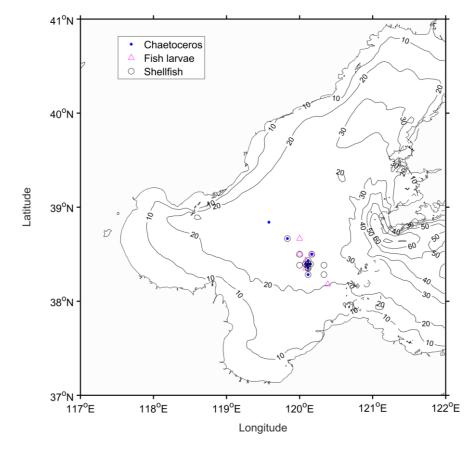

Figure 1. Distribution of sampling stations in the Bohai Sea in 2011. The dot, triangle and circle denote sampling stations of *Chaetoceros*, fish larvae and shellfish, respectively.

2.2. Radial Basis Function Interpolation

In order to analyze the effects of the oil spill on the distribution of organisms, the scatted observation data of *Chaetoceros,* shellfish and TPH is interpolated, with the the grid spacing of 10″ × 10″. Some interpolation methods, such as the Kriging, Cressman and RBF interpolations, have been proposed to alleviate this issue. Based on various interpolation methods, comparatively accurate and sufficient data are obtained in the field of marine science [44]. The interpolation method in this study is RBF interpolation, which is a well-established tool with high accuracy and numerical stability [45–47].

Assuming that there are n_i given points, $i = 1,2, \ldots , m$, the unknown point Z_{sd} is calculated by RBF interpolation:

$$Z_{sd}(x_j, y_j) = \sum_{i=1}^{n} c_i U(r_{ij}) + \lambda_1 + \lambda_2 x_i + \lambda_3 y_i \tag{1}$$

where r_{ij} is the Euclidean distance between $(x_i, \ y_i)$ and $(x_j, \ y_j)$, $U(r_{ij})$ is the basis function:

$$\begin{bmatrix} c \\ \lambda \end{bmatrix} = \begin{bmatrix} A & P \\ P^T & 0 \end{bmatrix}^{-1} \cdot \begin{bmatrix} Z \\ 0 \end{bmatrix} \tag{2}$$

$$c = \begin{bmatrix} c_1 \\ c_2 \\ \cdot \\ \cdot \\ \cdot \\ c_n \end{bmatrix}, \lambda = \begin{bmatrix} \lambda_1 \\ \lambda_2 \\ \lambda_3 \end{bmatrix}, P = \begin{bmatrix} 1 & x_1 & y_1 \\ 1 & x_2 & y_2 \\ \cdot & \cdot & \cdot \\ \cdot & \cdot & \cdot \\ \cdot & \cdot & \cdot \\ 1 & x_n & y_n \end{bmatrix}, Z = \begin{bmatrix} Z_{sd}(x_1, y_1) \\ Z_{sd}(x_2, y_2) \\ \cdot \\ \cdot \\ \cdot \\ Z_{sd}(x_n, y_n) \end{bmatrix} \tag{3}$$

$$A = \begin{bmatrix} 0 & U(r_{12}) & U(r_{13}) \cdots U(r_{1n}) \\ U(r_{21}) & 0 & U(r_{23}) \cdots U(r_{2n}) \\ & \cdot & \cdot & \cdot \\ & \cdot & \cdot & \cdot \\ & \cdot & \cdot & \cdot \\ U(r_{n1}) & U(r_{n2}) & U(r_{n3}) \ \cdots \ 0 \end{bmatrix} \tag{4}$$

Note that, linear radial basis functions are used in this paper:

$$U(r_{ij}) = r_{ij} \tag{5}$$

Table 1. Observation information of *Chaetoceros*, fish larvae and shellfish: location and date.

Chaetoceros			Fish Larvae			Shellfish		
Longitude (°N)	Latitude (°E)	Date	Longitude (°N)	Latitude (°E)	Date	Longitude (°N)	Latitude (°E)	Date
120.1164	38.2833	15 June	120.0831	38.35	21 June	120	38.5	16 June
120.1164	38.35	15 June	120.3839	38.1806	21 June	120.1667	38.5	16 June
120.1014	38.3844	15 June	120.0831	38.4333	22 June	120.0831	38.3956	16 June
120.0831	38.3956	16 June	120	38.5	28 June	120.1164	38.4333	16 June
120.1164	38.4333	16 June	120.1667	38.5	28 June	120.1014	38.3844	15 June
120.1667	38.5	16 June	120	38.6667	29 June	120.1164	38.35	15 June
120.1497	38.3956	16 June	120.0831	38.4333	13 July	120.1164	38.2833	15 June
120.1164	38.2833	21 June	120.0831	38.35	13 July	119.8333	38.6667	28 June
120.1164	38.35	21 June	120.3839	38.1806	13 July	120	38.5	28 June
120.1164	38.3956	21 June	120	38.5	14 July	120.1667	38.5	28 June
120.1133	38.3583	21 June	120.1667	38.5	14 July	120.0831	38.3956	22 June
119.5797	38.8403	24 June	120	38.6667	16 July	120.1164	38.4333	22 June
119.8333	38.6667	28 June				120.1164	38.3956	21 June
						120.1164	38.35	21 June
						120.1497	38.3956	22 June
						120.1164	38.2833	21 June
						120.	38.3833	28 June
						120.3333	38.3833	22 June
						120.3333	38.2833	21 June
						120.1133	38.3583	21 June

2.3. Oil Transport Model

In this paper, an adjoint assimilation model of oil transport is established to simulate the spatial and temporal distribution of TPH after the oil spill based on the observation data of the oil spill in the Bohai Sea. The observed data used in the model correspond to the period from June 2011 to July 2011, when petroleum hydrocarbon samples were collected on the sea surface in the Bohai Sea (Figure 2). The model can obtain satisfactory results and reduce the error by adjusting control variables and optimizing simulation results iteratively. The monitoring data of different time and space dynamically is fitted, considering the hydrodynamic process. The model assimilates the monitoring data of different time and space to the same time through the numerical iteration process of the monitoring values.
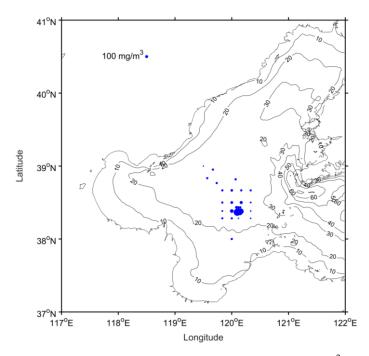
Figure 2. Location of the TPH sampling stations (unit: mg/m^3).

The adjoint assimilation model is based on the rectangular coordinates, where the parameters settings refer that in Wang et al. (2013) [48]. The computing area spans over the domain of 117.5° E~122.5° E and 37° N~41° N, with the grid spacing of 4′ × 4′. The model is divided into five layers vertically, whose thicknesses are 10 m, 10 m, 10 m, 20 m and 25 m from top to bottom, respectively. The time step is set as 1 h.

The flow field (Figure 3) which forces the oil transport model is calculated with the Finite-Volume Coastal Ocean Model (FVCOM). The computational domain is the Bohai Sea (117.5° E~122.5° E, 37° N~41° N), and the horizontal resolution is 1/24° in both latitude and longitude. The parameters of temperature and salinity are kept consistent with Chen et al. [49].
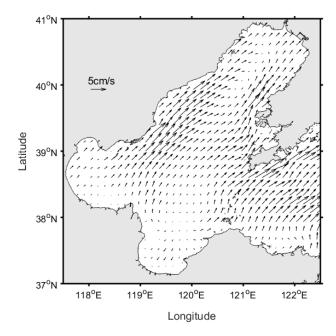

Figure 3. The surface flow field of the Bohai Sea at 0:00 am 1 June 2011.

Considering the convection and diffusion processes, the governing equation of the marine oil transport model is presented as follows:

$$\frac{\partial C}{\partial t} + u\frac{\partial C}{\partial x} + v\frac{\partial C}{\partial y} + w\frac{\partial C}{\partial z} = \frac{\partial}{\partial x}\left(A_H\frac{\partial C}{\partial x}\right) + \frac{\partial}{\partial y}\left(A_H\frac{\partial C}{\partial y}\right) + \frac{\partial}{\partial z}\left(K_H\frac{\partial C}{\partial z}\right) \tag{6}$$

where C denotes the concentration of TPH; t is the time; x, y, z are components of the Cartesian coordinate system in the eastern, northern and vertical direction, respectively; u, v, w are velocities in the x, y, z directions, respectively; A_H and K_H denote the horizontal and vertical diffusion coefficients, which are set as 100 m^2 s^{-1} and 10^{-5} m^2 s^{-1}, respectively. The equations of the adjoint model are presented in Appendix A.

3. Results and Discussion

3.1. Average Abundances of Chaetoceros, Fish Larvae, and Shellfish

The abundances of *Chaetoceros* and shellfish before and after the oil spill are shown in Figure 4. The average abundance is calculated as follows:

$$\overline{C} = \frac{1}{n}\sum_{i=1}^{n} C_i \tag{7}$$

where $\overline{C}$ is the average abundance. C_i is the observation abundance at the ith sampling stations. n denotes the number of sampling stations.
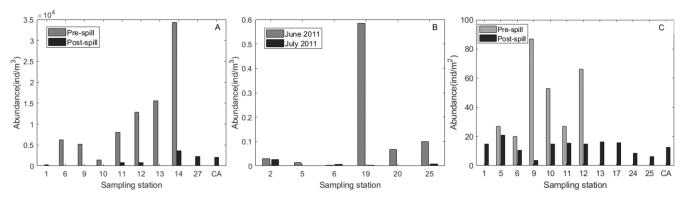

Figure 4. Abundance of *Chaetoceros* (**A**), Fish larvae (**B**), and Shellfish (**C**) at sampling stations.

The average abundances of *Chaetoceros* and shellfish before the oil spill are 11,941 ind/m^3 and 47 ind/m^2, respectively. While that after the oil spill are 1651 ind/m^3 and 12.1 ind/m^2, respectively. In addition, the average abundance of fish larvae in June and July is 0.13 ind/m^3 and 0.007 ind/m^3, respectively. According to the information of observation (Table 1), *Chaetoceros* and shellfish were observed before and after the oil spill, fish larvae was observed after the spill in June and July. By comparing the abundance before and after the oil spill, it is found that *Chaetoceros* and shellfish decreased significantly in the short term after the oil spill. The oil pollution also had a negative impact on fish larvae.

The effects of oil spills on marine organisms are still unclear and many findings often contradict each other (Table 2). Most investigations have reported that oil spills had negative effects on planktonic species, while a few investigations reported that spills had no significant effects on plankton. In our study, *Chaetoceros*, fish larvae and shellfish decreased significantly due to oil pollution, which is consistent with most of the previous reports. Compared with the previous study, for example, Peterson found phytoplankton first decreased and then followed by blooms [9]. Our result is consistent with the "first decreased", because the observation time in this study is only a few days after the oil spill.

As for the effects of zooplankton and zoobenthos, both the previous reports and our result showed that they could be affected by oil spills.

Table 2. Some marine oil spills reported and their implicit effects.

Name	Start Time	Location	Volume Spilled	Effects
Ixtoc I	3 June 1979	Bay of Campeche, Mexico	457,000–1,400,000 tonnes	The organization and structure of the zooplankton community changed after the spill [50].
Exxon Valdez	24 March 1989	Prince William Soumd, Alaska, USA	35,000 tonnes	Phytoplankton first decreased and then followed by blooms [9].
Sea Empress	15 February 1996	Milford Haven Wales	72,000 tonnes	Spill had no significant effects on the plankton [11].
Jessica	16 January 2001	Galapagos Islands	240,000 tonnes	Chlorophyll declined in the week directly following the spill, yet rose in the successive month to levels [12].
Prestige	13 November 2002	Off the Galician coast, Spain	63,000 tonnes	No noticeable changes in phytoplankton primary production and phytoplankton biomass [51].
Cosco Busan	7 November 2007	San Francisco Bay	54,000 gallons	Spill induced high mortality of herring eggs [18].
Deepwater Horizon Oil Spill	20 April 2010	Northern Gulf of Mexico	4.9 million gallons	The community structure was significantly changed, with a 38% decline in species richness and 26% decline in Shannon-Weiner diversity [20].
Penglai 19-3	June 2011 (a series of spills)	Bohai Sea	723 barrels (reported)	Oil spill caused abnormal chlorophyll concentration distributions and red tide nearby area of oil spill [17].

3.2. Variation in the Abundance of Chaetoceros, Fish Larvae, and Shellfish

Oil pollution results in the massive loss of *Chaetoceros*, fish larvae and shellfish. Mortality, which is the ratio of the total number of organisms that died in a period of time to the initial value, is used to measure the effect of oil pollution. To explore the relationship between the mortality and TPH, the mortality of *Chaetoceros*, fish larvae, and shellfish and TPH are fitted through the least-squares method (Figure 5). After the oil spill, the four-day mortality of *Chaetoceros*, fish larvae and shellfish ranged from 89.4% to 90.0%, 91.9% to 100% and 47.5% to 95.9%, respectively, indicating that oil pollution caused a negative impact on the growth of marine organisms. The mortality of shellfish is lower than that of *Chaetoceros* and fish larvae, suggesting that shellfish are less vulnerable to oil pollution as they live in the seabed while *Chaetoceros* and fish larvae live in surface waters. Furthermore, the mortality of fish larvae is positively correlated with TPH concentration while the mortality of shellfish is negatively correlated with TPH. However, due to the limitation of data, the complicated mechanism behind the negative correlation needs to be further explored.

According to the water quality standards in China, when the concentration of TPH is above 50 mg/m^3, TPH may cause ecological damage to different species of marine organisms. Calculations showed that the four-day mortality of *Chaetoceros* is over 90% and shellfish is over 78.9% by calculation when the concentration of TPH exceeds the water quality standards in China, suggesting the TPH has a significant ecological damage. Mortality is the ratio of the total number of organisms that died in a period of time to the initial value. In order to explore the daily variation of the abundance after the oil spill, the daily mortality for *Chaetoceros* and shellfish are calculated based on the four-day mortality (90%, 78.9%). In short, when the TPH concentration is over 50 mg/m^3, the daily mortality of *Chaetoceros* is over 43.8% and shellfish is over 32.3%.
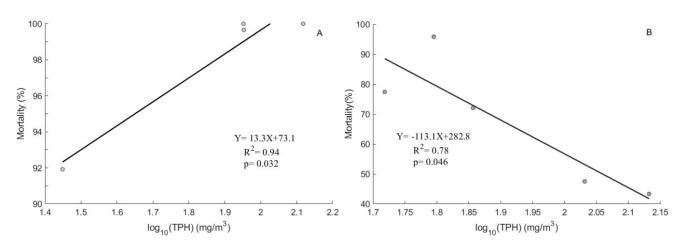
Figure 5. Relationship between the TPH and the Mortality of fish larvae (**A**), shellfish (**B**). The concentration of TPH is reduced by natural logarithm.

Ainsworth et al. observed that the biomass of large reef fish decreased by 25% to 50% in areas most affected by a spill, and biomass of large demersal fish decreased even more, by 40% to 70% [52]. This biomass decrease is different from our result, probably because the observation time of data is different.

3.3. Spatial Distribution of the Mortality and the Death Rate

The spatial distribution of *Chaetoceros* (Figure 6) and TPH (Figure 7A) are obtained by RBF interpolation, and the spatial distribution of *Chaetoceros* mortality (Figure 7C) and death rate (Figure 7B) are also obtained. According to the interpolation result, the average abundance of *Chaetoceros* is 12,001 ind/m^3, and the death rate is positively correlated with TPH, with a correlation coefficient of 0.70. However, the correlation between the mortality and TPH is not significant. The equations of mortality and death rate are presented in Appendix B.
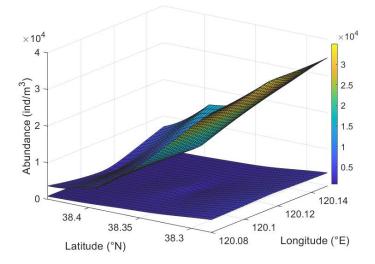

Figure 6. Distribution of the interpolated *Chaetoceros* concentration. The upper layer is on 15 June, and the lower layer is on 21 June.
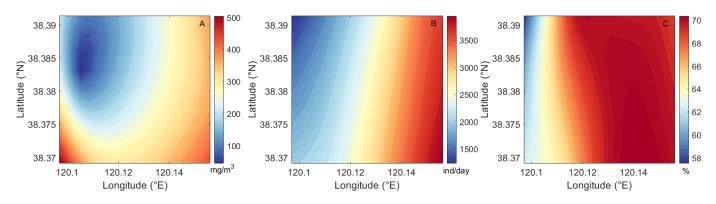
Figure 7. Distribution of the interpolated TPH concentration (**A**), death rate (**B**) and mortality (**C**) of *Chaetoceros* on 18 June.

The distribution of shellfish is shown in Figure 8. The average abundance of shellfish is 43 ind/m^2. The death rate of shellfish is positively correlated with TPH (Figure 9), with the correlation coefficient of 0.91. While the correlation between the mortality of shellfish and TPH is not significant, which is similar to *Chaetoceros*.
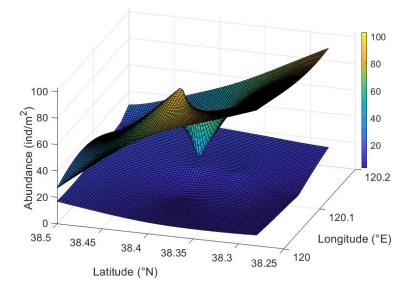

Figure 8. Distribution of the interpolated shellfish concentration. The upper layer is on 15 June, and the lower layer is on 21 June.
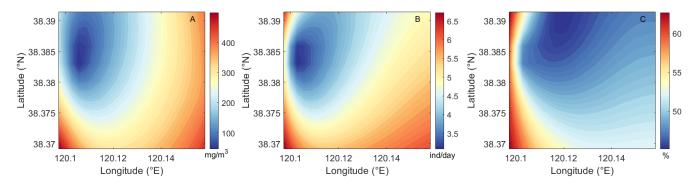

Figure 9. Distribution of the interpolated TPH concentration (**A**), death rate (**B**) and mortality (**C**) of Shellfish on 18 June.

3.4. General Evaluation of the Biomass Loss

The daily mean distribution of TPH is obtained by the adjoint assimilation model. After assimilation, the mean absolute error of concentration decreases from 57.02 mg/m^3 to 28.53 mg/m^3, with a decreasing ratio of about 50%. According to the water quality standards in China, an area with the concentration of TPH over 50 mg/m^3 is considered to be toxic. The spatial distribution of TPH from June 18 to June 21 indicates that the range of the high concentration area decreases (Figure 10).
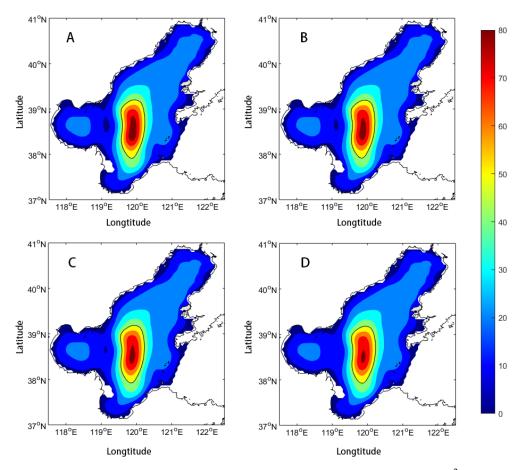

Figure 10. Daily change of the TPH distribution from June 18 to June 21 (unit: mg/m^3). Contour line for 50 mg/m^3 is shown as black curved line. The mean distribution of TPH on June 18, June 19, June 20 and June 21 is shown in (**A**–**D**), respectively.

Chaetoceros and shellfish were observed pre-spill and post-spill, but fish larvae were only observed after the oil spill. Thus, the data of *Chaetoceros* and Shellfish were used to evaluate the biomass loss combined with the distribution of TPH obtained by the adjoint assimilation model. According to the water quality standards in China, the mortality of *Chaetoceros* and shellfish are estimated so as to comprehensively evaluate the loss of *Chaetoceros* and shellfish during the observation period. Based on the average value of observation data (*Chaetoceros*: 11,941 ind/m^3; shellfish: 47 ind/m^2), the total loss of *Chaetoceros* and shellfish in toxic area are 7.25×10^{14} ind and 2.51×10^5 ind, respectively (Table 3). While, according to the interpolation result, the total loss of *Chaetoceros* and shellfish are 7.28×10^{14} ind and 2.30×10^5 ind, respectively. The comparison indicates that the total death of *Chaetoceros* and shellfish calculated based on the interpolation are close to those of the observation data. Combining these two results, the total death of *Chaetoceros* is $7.25 \times 10^{14} \sim 7.28 \times 10^{14}$ ind and shellfish is $2.30 \times 10^{12} \sim 2.51 \times 10^{12}$ ind during the observation period.

Table 3. The daily death and the total death of *Chaetoceros* and shellfish from June 18 to June 21 based on observation data and interpolation result.

Date	Based on Observation Data		Based on Interpolation Result	
	Chaetoceros ($\times 10^{14}$ ind)	Shellfish ($\times 10^{11}$ ind)	*Chaetoceros* ($\times 10^{14}$ ind)	Shellfish ($\times 10^{11}$ ind)
18 June	3.51	10.1	3.53	9.32
19 June	2.01	7.08	2.02	6.48
20 June	1.10	4.61	1.10	4.22
21 June	0.63	3.25	0.63	2.98

4. Conclusions

Oil spills can cause marine environmental pollution, resulting in a decline of marine ecosystem services function. The Penglai 19-3 oil spill is one of the typical oil spills in the Bohai Sea. The assessment of ecological loss following the oil spill based on observation data is however limited at present. In this paper, based on the observation data of *Chaetoceros*, fish larvae and shellfish near the platform C of the Penglai 19-3 drilling field, the negative effect of oil spill on biological growth is evaluated, and the damage of biological resources caused by oil spill accident is estimated. The oil spill caused the biomass loss of *Chaetoceros*, fish larvae and shellfish.

According to the observation data, the average abundances of *Chaetoceros* and shellfish before the oil spill were 11,941 ind/m^3 and 47 ind/m^2, and after the oil spill were 1651 ind/m^3 and 12.1 ind/m^2, respectively. The average abundance of fish larvae in June and July were 0.13 ind/m^3 and 0.007 ind/m^3, respectively. The abundances of all these three organisms decrease in large quantities in the short term after the oil spill. The four-day mortality of *Chaetoceros* and fish larvae was around 90%, and that of shellfish was 78.9%, which is lower than that of *Chaetoceros* and fish larvae. It can be obtained that the daily mortality of *Chaetoceros* and shellfish were 43.8% and 32.3%, respectively. The spatial distribution of the death rate, mortality and TPH are obtained through RBF interpolation. According to the result, the average abundances of *Chaetoceros* and shellfish were 12,001 ind/m^3 and 43 ind/m^2 and the death rate of *Chaetoceros* and shellfish are both positively correlated with TPH. However, the correlation between the mortality and TPH is not significant.

In order to evaluate the total loss of organisms, the temporal and spatial distribution of TPH is obtained by assimilating the monitoring data of TPH through the oil spill adjoint model. Based on the spatial and temporal distribution field, the area within the concentration of TPH over the water quality standards in China (50 mg/m^3) is obtained. According to the daily mortality and the reference value (the average abundance before oil spill based on the observation data and RBF interpolation result), the total losses of *Chaetoceros* and shellfish caused by the oil spill were $7.25 \times 10^{14} \sim 7.28 \times 10^{14}$ ind and $2.30 \times 10^{12} \sim 2.51 \times 10^{12}$ ind in the area where the TPH was over 50 mg/m^3 during the observation period.

In this paper, *Chaetoceros*, fish larvae and shellfish served as the indicators of risk to assess the damage of marine ecological resources caused by an oil spill, which is useful in future environmental monitoring efforts regarding pollution. The results of this study also highlight the necessity of early monitoring and sampling efforts shortly after the occurrence of oil spills. Understanding the alterations to organism community structure which can ultimately affect the higher trophic levels in these ecosystems can permit an improved assessment of the short-term influence of an oil spill on the marine ecosystem.

Author Contributions: Conceptualization, X.L.; Formal analysis, S.L.; Funding acquisition, X.L.; Investigation, H.H.; Methodology, H.H.; Software, H.H. and S.H.; Supervision, X.L.; Writing-original draft, H.H.; Writing-review & editing, J.S. All authors have read and agreed to the published version of the manuscript.

Appendix A. Adjoint Model

The adjoint assimilation model based on Lagrange multiplier method is used to simulate the spatial and temporal distribution of the total petroleum hydrocarbons (TPH) in the Bohai Sea, and the cost function representing the difference between the observation and the simulation results was constructed:

$$J = \frac{1}{2} \sum K_C \left(C_{i,j,k} - \overline{C}_{i,j,k} \right)^2 \tag{A1}$$

where $C_{i,j,k}$ and $\overline{C}_{i,j,k}$ are the simulated and the observed TPH data, respectively. K_C represents the weighting matrix whose element equals to 1 when the observations are available; otherwise, $K_C = 0$.

The construction of the Lagrange function is as follows:

$$L(C^*, C) = \int_\Omega C^* \left[\frac{\partial C}{\partial t} + u \frac{\partial C}{\partial x} + v \frac{\partial C}{\partial y} + w \frac{\partial C}{\partial z} - \frac{\partial}{\partial x} \left(A_H \frac{\partial C}{\partial x} \right) - \frac{\partial}{\partial y} \left(A_H \frac{\partial C}{\partial y} \right) - \frac{\partial}{\partial z} \left(K_H \frac{\partial C}{\partial z} \right) \right] d\Omega + J(C) \tag{A2}$$

where C^* represents the adjoint variable of C, according to the Lagrange multiplier method:

$$\frac{\partial L}{\partial C^*} = 0 \tag{A3}$$

$$\frac{\partial L}{\partial C} = 0 \tag{A4}$$

The adjoint equation can be obtained from (6):

$$-\frac{\partial C^*}{\partial t} - \frac{\partial C}{\partial z} \left(K_H \frac{\partial C}{\partial z} \right) = \frac{\partial (u C^*)}{\partial x} + \frac{\partial (v C^*)}{\partial y} + \frac{\partial (w C^*)}{\partial z} + \frac{\partial}{\partial x} \left(A_H \frac{\partial C^*}{\partial x} \right) + \frac{\partial}{\partial y} \left(A_H \frac{\partial C^*}{\partial y} \right) - K_c (C - \overline{C}) \tag{A5}$$

The gradient expression of the cost function regarding the initial TPH field can be derived from (7):

$$\frac{\partial J}{\partial C} = \frac{\partial C^*}{\partial t} + \frac{\partial (u C^*)}{\partial x} + \frac{\partial (v C^*)}{\partial y} + \frac{\partial (w C^*)}{\partial z} + \frac{\partial}{\partial x} \left(A_H \frac{\partial C^*}{\partial x} \right) + \frac{\partial}{\partial y} \left(A_H \frac{\partial C^*}{\partial y} \right) + \frac{\partial}{\partial z} \left(K_H \frac{\partial C^*}{\partial y} \right) \tag{A6}$$

Appendix B. Definition of the Mortality, Death Rate and Daily Death

Mortality in this paper is defined as follows:

$$m(x, y, t) = \frac{f(x, y, t - \Delta t) - f(x, y, t + \Delta t)}{f(x, y, t - \Delta t)} \tag{A7}$$

Death rate in this paper is defined as follows:

$$d(x, y, t) = \frac{f(x, y, t - \Delta t) - f(x, y, t + \Delta t)}{2\Delta t} \tag{A8}$$

where $f(x, y, t)$ is abundance of organism and Δt is 48 h. The daily death can be calculated as follows:

The total death of the first day:

$$Cq \tag{A9}$$

The total death of the second day:

$$Cq - Cq^2 \tag{A10}$$

The total death of the third day:

$$Cq^3 - 2Cq^2 + Cq \tag{A11}$$

The total death of the fourth day:

$$-Cq^4 + 3Cq^3 - 3Cq^2 + Cq \tag{A12}$$

Thus, the final mortality is:

$$-q^4 + 3q^3 - 3q^2 + q \tag{A13}$$

where *q* is the initial mortality and *C* is initial abundance of organism.

References

1. Brussaard, C.P.D.; Peperzak, L.; Beggah, S.; Wick, L.Y.; Wuerz, B.; Weber, J.; Samuel Arey, J.; Van der Burg, B.; Jonas, A.; Huisman, J.; et al. Immediate ecotoxicological effects of short-lived oil spills on marine biota. *Nat. Commun.* **2016**, *7*, 11206. [CrossRef]
2. González, J.; Figueiras, F.G.; Aranguren-Gassis, M.; Crespo, B.G.; Fernández, E.; Morán, X.A.G.; Nieto-Cid, M. Effect of a simulated oil spill on natural assemblages of marine phytoplankton enclosed in microcosms. *Estuar. Coast. Shelf Sci.* **2009**, *83*, 265–276. [CrossRef]
3. D'Adamo, R.; Pelosi, S.; Trotta, P.; Sansone, G. Bioaccumulation and biomagnification of polycyclic aromatic hydrocarbons in aquatic organisms. *Mar. Chem.* **1997**, *56*, 45–49. [CrossRef]
4. Wang, X.; Wang, W.X. Bioaccumulation and transfer of benzo(a)pyrene in a simplified marine food chain. *Mar. Ecol. Prog. Ser.* **2006**, *312*, 101–111. [CrossRef]
5. González, J.J.; Viñas, L.; Franco, M.A.; Fumega, J.; Soriano, J.A.; Grueiro, G.; Muniategui, S.; López-Mahía, P.; Prada, D.; Bayona, J.M.; et al. Spatial and temporal distribution of dissolved/dispersed aromatic hydrocarbons in seawater in the area affected by the Prestige oil spill. *Mar. Pollut. Bull.* **2006**, *53*, 250–259. [CrossRef]
6. Hjorth, M.; Forbes, V.E.; Dahllöf, I. Plankton stress responses from PAH exposure and nutrient enrichment. *Mar. Ecol. Prog. Ser.* **2008**, *363*, 121–130. [CrossRef]
7. Andres, B.A. The Exxon valdez Oil Spill Disrupted the Breeding of Black Oystercatchers. *J. Wildl. Manage.* **1997**, *61*, 1322–1328. [CrossRef]
8. Lamont, M.M.; Carthy, R.R.; Fujisaki, I. Declining reproductive parameters highlight conservation needs of loggerhead turtles (Caretta caretta) in the Northern Gulf of Mexico. *Chelonian Conserv. Biol.* **2012**, *11*, 190–196. [CrossRef]
9. Peterson, C.H.; Rice, S.D.; Short, J.W.; Esler, D.; Bodkin, J.L.; Ballachey, B.E.; Irons, D.B. Long-Term Ecosystem Response to the Exxon Valdez Oil Spill. *Science* **2003**, *302*, 2082–2086. [CrossRef]
10. Klemas, V. Tracking Oil Slicks and Predicting their Trajectories Using Remote Sensors and Models: Case Studies of the Sea Princess and Deepwater Horizon Oil Spills. *J. Coast. Res.* **2010**, *26*, 789–797. [CrossRef]
11. Batten, S.D.; Allen, R.J.S.; Wotton, C.O.M. The effects of the Sea Empress oil spill on the plankton of the southern Irish Sea. *Mar. Pollut. Bull.* **1998**, *36*, 764–774. [CrossRef]
12. Banks, S. SeaWiFS satellite monitoring of oil spill impact on primary production in the Galápagos Marine Reserve. *Mar. Pollut. Bull.* **2003**, *47*, 325–330. [CrossRef]
13. Lee, C.I.; Kims, M.C. Temporal variation in the chlorophyll a concentration of the coastal waters of Spain following the ship Prestige oil spill. *J. Fish. Sci. Technol.* **2008**, *11*, 212–218. [CrossRef]
14. Lee, C.I.; Kim, M.C.; Kim, H.C. Temporal variation of chlorophyll a concentration in the coastal waters affected by the Hebei Spirit oil spill in the West Sea of Korea. *Mar. Pollut. Bull.* **2009**, *58*, 496–502. [CrossRef]
15. Sheng, Y.; Tang, D.; Pan, G. Phytoplankton bloom over the Northwest Shelf of Australia after the Montara oil spill in 2009. *Geomat. Nat. Hazards Risk* **2011**, *2*, 329–347. [CrossRef]
16. Ohwada, K.; Nishimura, M.; Wada, M.; Nomura, H.; Shibata, A.; Okamoto, K.; Toyoda, K.; Yoshida, A.; Takada, H.; Yamada, M. Study of the effect of water-soluble fractions of heavy-oil on coastal marine organisms using enclosed ecosystems, mesocosms. *Mar. Pollut. Bull.* **2003**, *47*, 78–84. [CrossRef]
17. Guo, J.; Liu, X.; Xie, Q. Characteristics of the Bohai Sea oil spill and its impact on the Bohai Sea ecosystem. *Chin. Sci. Bull.* **2013**, *58*, 2276–2281. [CrossRef]

18. Incardona, J.P.; Vines, C.A.; Anulacion, B.F.; Baldwin, D.H.; Day, H.L.; French, B.L.; Labenia, J.S.; Linbo, T.L.; Myers, M.S.; Olson, O.P.; et al. Unexpectedly high mortality in Pacific herring embryos exposed to the 2007 Cosco Busan oil spill in San Francisco Bay. *Proc. Natl. Acad. Sci. USA* **2012**, *109*, E51–E58. [CrossRef] [PubMed]

19. Brannon, E.L.; Collins, K.; Cronin, M.A.; Moulton, L.L.; Maki, A.L.; Parker, K.R. Review of the Exxon Valdez oil spill effects on pink salmon in Prince William Sound, Alaska. *Rev. Fish. Sci.* **2012**, *20*, 20–60. [CrossRef]

20. Lewis, J.P.; Tarnecki, J.H.; Garner, S.B.; Chagaris, D.D.; Patterson, W.F. Changes in Reef Fish Community Structure Following the Deepwater Horizon Oil Spill. *Sci. Rep.* **2020**, *10*, 5621. [CrossRef] [PubMed]

21. Gesteira, J.L.G.; Dauvin, J.C. Amphipods are good bioindicators of the impact of oil spills on soft-bottom macrobenthic communities. *Mar. Pollut. Bull.* **2000**, *40*, 1017–1027. [CrossRef]

22. Faghihifard, M.; Badri, M.A. Simulation of oil pollution in the Persian Gulf near Assaluyeh oil terminal. *Mar. Pollut. Bull.* **2016**, *105*, 143–149. [CrossRef]

23. Zhang, J.; Kitazawa, D. Numerical analysis of particulate organic waste diffusion in an aquaculture area of Gokasho Bay, Japan. *Mar. Pollut. Bull.* **2015**, *93*, 130–143. [CrossRef] [PubMed]

24. Wang, S.D.; Shen, Y.M.; Guo, Y.K.; Tang, J. Three-dimensional numerical simulation for transport of oil spills in seas. *Ocean Eng.* **2008**, *35*, 503–510. [CrossRef]

25. Abascal, A.J.; Castanedo, S.; Medina, R.; Liste, M. Analysis of the reliability of a statistical oil spill response model. *Mar. Pollut. Bull.* **2010**, *60*, 2099–2110. [CrossRef] [PubMed]

26. Alves, T.M.; Kokinou, E.; Zodiatis, G.; Lardner, R.; Panagiotakis, C.; Radhakrishnan, H. Modelling of oil spills in confined maritime basins: The case for early response in the Eastern Mediterranean Sea. *Environ. Pollut.* **2015**, *206*, 390–399. [CrossRef]

27. Alves, T.M.; Kokinou, E.; Zodiatis, G.; Radhakrishnan, H.; Panagiotakis, C.; Lardner, R. Multidisciplinary oil spill modeling to protect coastal communities and the environment of the Eastern Mediterranean Sea. *Sci. Rep.* **2016**, *6*, 36882. [CrossRef] [PubMed]

28. Lawson, L.M.; Hofmann, E.E.; Spitz, Y.H. Time series sampling and data assimilation in a simple marine ecosystem model. *Deep. Res. Part II Top. Stud. Oceanogr.* **1996**, *43*, 625–651. [CrossRef]

29. Gunson, J.; Oschlies, A.; Garçon, V. Sensitivity of ecosystem parameters to simulated satellite ocean color data using a coupled physical-biological model of the North Atlantic. *J. Mar. Res.* **1999**, *57*, 613–639. [CrossRef]

30. Fennel, K.; Losch, M.; Schroter, J.; Wenzel, M. Testing a marine ecosystem model: Sensitivity analysis and parameter optimization. *J. Mar. Syst.* **2001**, *28*, 45–63. [CrossRef]

31. Friedrichs, M.A.M. A data assimilative marine ecosystem model of the central equatorial Pacific: Numerical twin experiments. *J. Mar. Res.* **2001**, *59*, 859–894. [CrossRef]

32. Zhao, L.; Wei, H.; Xu, Y.; Feng, S. An adjoint data assimilation approach for estimating parameters in a three-dimensional ecosystem model. *Ecol. Modell.* **2005**, *186*, 235–250. [CrossRef]

33. Zhang, L.; Constantinescu, E.M.; Sandu, A.; Tang, Y.; Chai, T.; Carmichael, G.R.; Byun, D.; Olaguer, E. An adjoint sensitivity analysis and 4D-Var data assimilation study of Texas air quality. *Atmos. Environ.* **2008**, *42*, 5787–5804. [CrossRef]

34. Gao, X.; Wei, Z.; Lv, X.; Wang, Y.; Fang, G. Numerical study of tidal dynamics in the South China Sea with adjoint method. *Ocean Model.* **2015**, *92*, 101–114. [CrossRef]

35. Kuroda, H.; Kishi, M.J. A data assimilation technique applied to estimate parameters for the NEMURO marine ecosystem model. *Ecol. Modell.* **2004**, *172*, 69–85. [CrossRef]

36. Zong, X.; Xu, M.; Xu, J.; Lv, X. Improvement of the ocean pollutant transport model by using the surface spline interpolation. *Tellus A Dyn. Meteorol. Oceanogr.* **2018**, *70*, 1–13. [CrossRef]

37. Li, X.; Zheng, Q.; Lv, X. Application of the spline interpolation in simulating the distribution of phytoplankton in a marine npzd type ecosystem model. *Int. J. Environ. Res. Public Health* **2019**, *16*, 2664. [CrossRef] [PubMed]

38. Zheng, Q.; Li, X.; Lv, X. Application of dynamically constrained interpolation methodology to the surface nitrogen concentration in the Bohai sea. *Int. J. Environ. Res. Public Health* **2019**, *16*, 2400. [CrossRef] [PubMed]

39. Huang, S.; Han, H.; Li, X.; Song, D.; Shi, W.; Zhang, S.; Lv, X. Inversion of the Degradation Coefficient of Petroleum Hydrocarbon Pollutants in Laizhou Bay. *J. Mar. Sci. Eng.* **2021**, *9*, 655. [CrossRef]

40. Nomura, H.; Toyoda, K.; Yamada, M.; Okamoto, K.; Wada, M.; Nishimura, M.; Yoshida, A.; Shibata, A.; Takada, H.; Ohwada, K. Mesocosm studies on phytoplankton community succession after inputs of the water-soluble fraction of Bunker A oil. *La Mer* **2007**, *45*, 105–116.

41. Vikebø, F.B.; Rønningen, P.; Meier, S.; Grøsvik, B.E.; Lien, V.S. Dispersants have limited effects on exposure rates of oil spills on fish eggs and larvae in shelf seas. *Environ. Sci. Technol.* **2015**, *49*, 6061–6069. [CrossRef] [PubMed]

42. Zhou, H.; Zhang, Z.; Liu, X.; Hua, E. Decadal change in sublittoral macrofaunal biodiversity in the Bohai Sea, China. *Mar. Pollut. Bull.* **2012**, *64*, 2364–2373. [CrossRef] [PubMed]

43. Guo, M.; Zheng, G.; Peng, J.; Meng, D.; Wu, H.; Tan, Z.; Li, F.; Zhai, Y. Distribution of perfluorinated alkyl substances in marine shellfish along the Chinese Bohai Sea coast. *J. Environ. Sci. Health Part B* **2019**, *54*, 271–280. [CrossRef]

44. Liu, Y.; Yu, J.; Shen, Y.; Lv, X. A modified interpolation method for surface total nitrogen in the Bohai Sea. *J. Atmos. Ocean. Technol.* **2016**, *33*, 1509–1517. [CrossRef]

45. Morse, B.S.; Yoo, T.S.; Rheingans, P.; Chen, D.T.; Subramanian, K.R. Interpolating implicit surfaces from scattered surface data using compactly supported radial basis functions. In *SIGGRAPH '05: ACM SIGGRAPH 2005 Courses*; ACM: New York, NY, USA, 2001; pp. 89–98.

46.   Hon, Y.C.; Schaback, R. On unsymmetric collocation by radial basis functions. *Appl. Math. Comput.* **2001**, *119*, 177–186. [CrossRef]

47.   Mishra, P.K.; Nath, S.K.; Sen, M.K.; Fasshauer, G.E. Hybrid Gaussian-cubic radial basis functions for scattered data interpolation. *Comput. Geosci.* **2018**, *22*, 1203–1218. [CrossRef]

48.   Wang, C.H.; Li, X.; Lv, X. Numerical Study on Initial Field of Pollution in the Bohai Sea with an Adjoint Method. *Math. Probl. Eng.* **2013**, *2013*, 104591. [CrossRef]

49.   Chen, C.; Liu, H.; Beardsley, R.C. An unstructured grid, finite-volume, three-dimensional, primitive equations ocean model: Application to coastal ocean and estuaries. *J. Atmos. Ocean. Technol.* **2003**, *20*, 159–186. [CrossRef]

50.   Próo, S.G.D.; Chávez, E.A.; Alatriste, F.M.; de la Campa, S.; de la Cruz, G.; Gómez, L.; Guadarrama, R.; Guerra, A.; Mille, S.; Torruco, D. The impact of the ixtoc-1 oil spill on zooplankton. *J. Plankton Res.* **1986**, *8*, 557–581. [CrossRef]

51.   Varela, M.; Bode, A.; Lorenzo, J.; Álvarez-Ossorio, M.T.; Miranda, A.; Patrocinio, T.; Anadón, R.; Viesca, L.; Rodríguez, N.; Valdés, L.; et al. The effect of the "Prestige" oil spill on the plankton of the N-NW Spanish coast. *Mar. Pollut. Bull.* **2006**, *53*, 272–286. [CrossRef]

52.   Ainsworth, C.H.; Paris, C.B.; Perlin, N.; Dornberger, L.N.; Patterson, W.F.; Chancellor, E.; Murawski, S.; Hollander, D.; Daly, K.; Romero, I.C.; et al. Impacts of the Deepwater Horizon oil spill evaluated using an end-to-end ecosystem model. *PLoS ONE* **2018**, *13*, e0190840.